

# Crosslinked blends of poly(lactic acid) and polyacrylates: AFM, DSC and XRD studies

Halina Kaczmarek · Marek Nowicki · Irena Vuković-Kwiatkowska · Sylwia Nowakowska

Received: 31 July 2012 / Accepted: 17 January 2013 / Published online: 5 February 2013  
© The Author(s) 2013. This article is published with open access at Springerlink.com

**Abstract** The blends based on poly(lactic acid), (PLA) and polyacrylates (1:1 weight ratio) have been prepared by photopolymerization of three different multifunctional acrylate monomers (pentaerythritol triacrylate, pentaerythritol tetraacrylate and dipentaerythritol pentaacrylate) in matrix of linear PLA. The structure of these systems has been studied by Atomic Force Microscopy (AFM), Differential Scanning Calorimetry (DSC) and X-ray Diffraction (XRD). It was found that the blends are highly crosslinked, rough, heterogeneous and some of them – semicrystalline. The effect of UV-irradiation on surface morphology of obtained mixtures was studied. The viscometry has been applied for measurements of changes of PLA molecular weight resulting of photodegradation. It was shown that blends are much more photostable than pure PLA.

**Keywords** Poly(lactic acid) · Polyacrylates · Blends · UV-irradiation · AFM · DSC · XRD

## Introduction

Poly(lactic acid) (PLA), which can be obtained from lactic acid (or lactide) formed in the process of starch fermentation is one of the promising future materials [1, 2]. PLA is environmentally friendly polymer owing to its biodegradability and biocompatibility. Moreover, it is a valuable

material in numerous applications (e.g. in packaging of food articles) thanks to its physicochemical properties. Nevertheless, this polymer also possesses some disadvantages, for example, high permeability of gases or vapors through PLA films. Thus, in the recent years, the great attention has been devoted to PLA modification leading to the improvement of barrier properties and extension of its application [3, 4].

There are few strategies of polymer modification – the changes of chemical structure in the bulk (i.e. in the whole material volume) or only at thin top layer. Both effects can be achieved by the chemical reactions (copolymerization, grafting, crosslinking, UV-irradiation, plasma treatment) or by physical factors (heating, physical blending with different modifiers) [4–7].

The studies of the surface properties are significant from the practical point of view. These properties determine the polymer behavior in the processes of adhesion, adsorption, permeation, catalysis, friction, wetting, printing etc. Among various experimental techniques allowing the characterization of the surface properties, the significance of AFM systematically increases [8–10]. Nowadays, AFM plays a key role in microelectronics, nano- and biotechnologies. The different modes (static and dynamic) are broadly applied in investigation of polymer blends, such as topographical and compositional mapping, in studies of molecules interactions, adhesion and mechanical behavior in nanometer scale.

The purpose of this work was to study the properties of blends based on poly(lactic acid) and polyacrylates by Atomic Force Microscopy (AFM), Differential Scanning Calorimetry (DSC) and X-Ray Diffraction (XRD). These compositions were prepared by photopolymerization of three multifunctional acrylate monomers in matrix of linear PLA. The details of synthesis kinetics of investigated blends have been recently published [11]. The effect of high energy ultraviolet irradiation on the properties of studied blends has been also presented.

H. Kaczmarek (✉) · I. Vuković-Kwiatkowska  
Faculty of Chemistry, Nicolaus Copernicus University,  
Gagarina 7 street,  
87-100 Toruń, Poland  
e-mail: halina@chem.uni.torun.pl

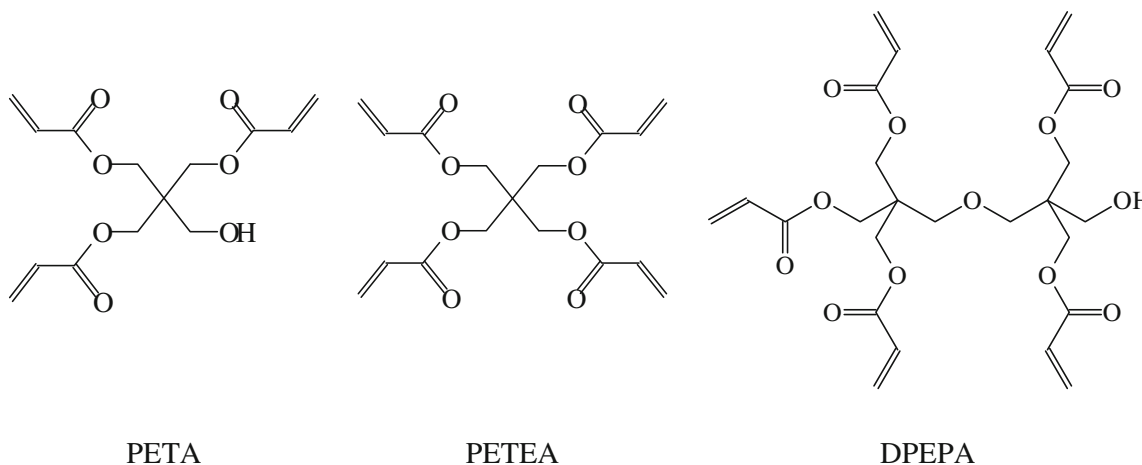
M. Nowicki · S. Nowakowska  
Institute of Physics, Poznań University of Technology,  
Nieszawska 13A street,  
60-965 Poznań, Poland

## Experimental

### Materials

Poly(lactic acid) (2002D type, Nature Works, USA) in the form of granules has been used in this work. Other reagents

were: pentaerythritol triacrylate (PETA), pentaerythritol tetraacrylate (PETEA), dipentaerythritol pentaacrylate (DPEPA) (Aldrich, USA), Darocur 1173 photoinitiator (Ciba, Switzerland) and chloroform as a solvent (POCH Spółka Akcyjna, Poland). The chemical structure formulae of applied monomers are given below:



Poly(lactic acid) has been purified by precipitation from solution. Next, the chloroform solution of pure PLA has been mixed with monomer and 5 % (wt) of photoinitiator. The weight ratio of monomer to polymer was 1:1. The solution was cast onto glass plates and dried at room temperature in the dark. After solvent removing, the specimens were cured by UV-light for 5 min.

### UV exposure

The high pressure mercury vapor lamp (HPK125W, Philips, Holland) has been used for photocuring of monomers at air atmosphere. The low pressure lamp TUV 30W, Philips has been applied to determine the photostability of cured blends.

The lamp emits polychromatic radiation (248–578 nm) which intensity was  $16.65 \text{ W/m}^2$ . The distance between sample and light source was 10 cm and temperature on the sample level was  $30 \text{ }^\circ\text{C}$ .

### Atomic force microscopy (AFM)

Intermittent-Contact Atomic Force Microscopy (IC-AFM) was applied for surface analysis. Scanning Probe Microscopy diInnova, Veeco, equipped in silicon cantilevers Nanosensors™ PPP-NCLR working in frequency of 146–

236 kHz and dynamic mode with phase contrast imaging has been used. The areas of three different sizes were scanned for all samples:  $10 \mu\text{m} \times 10 \mu\text{m}$ ,  $5 \mu\text{m} \times 5 \mu\text{m}$  and  $1 \mu\text{m} \times 1 \mu\text{m}$ . The results were analyzed using WSxM 5.0 Develop 1.2 software [12]. Sample roughness has been estimated on the base of arithmetic mean roughness ( $R_a$  parameter).

### Differential scanning calorimetry (DSC)

Differential Scanning Calorimetry measurements of pure PLA and obtained networks were performed on Diamond DSC power compensation type (Perkin-Elmer). All experiments were conducted at the heating and cooling rate of  $200 \text{ }^\circ\text{C/min}$ , under helium atmosphere with the flow rate of 20 ml/min, in the temperature range from  $-50$  to  $+220 \text{ }^\circ\text{C}$ . The instrument was calibrated using indium as a standard. The samples of about 5 mg were placed in aluminum pans. After the first heating run, the samples were cooled down, and subsequently heated again with same rate (i.e. so-called second run). After each run the samples were held for 3 min at a constant (minimal and maximal) temperature. The glass transition temperatures ( $T_g$ ) were determined from the second heating run while the melting has been discussed on the base of both: the first and the second runs.

## X-ray diffraction (XRD)

XRD patterns of all samples were recorded using XPERT PRO, Philips, operating at voltage of 40 kV, current - 30 mA; scanning speed -  $7.5 \cdot 10^{-3}$  °/s. The applied radiation from target CuK $\alpha$  was nickel filtered ( $\lambda=1.540$  Å). The range of scattering angles ( $2\theta$ ) was 5–40°. The obtained curves have been mathematically elaborated using Hpert High Score software. X-ray diffraction patterns were obtained at room temperature.

## Viscometry

The viscosity measurements of PLA were carried out in dilute chloroform solutions at constant temperature (25 °C) using an Ubbelohde viscometer. The time of liquid flow through the capillary has been measured with accuracy of 0.01 s. The limiting viscosity number (LVN,  $[\eta]$ ) was calculated by a double extrapolation using Huggins' and Kraemer equations. The viscosity average molecular weight has been obtained from Mark-Houwink Eq. (1):

$$[\eta] = K \cdot M_v^\alpha \quad (1)$$

where K and  $\alpha$  are constants were taken from reference [13]:

$$K = 2,21 \text{ E} - 04 [\text{cm}^3 \text{mol/g}^2]; \alpha = 0,77$$

Uncrosslinked residue of PLA from photodegraded composites has been extracted by chloroform and viscosity of solutions was measured.

Moreover, in UV-irradiated samples, the number of chain scission (S) per molecule has been calculated according to formula (2):

$$S = \left( \frac{[\eta]_0}{[\eta]_t} \right)^{1/\alpha} - 1 \quad (2)$$

where:  $[\eta]_0$  – LVN of PLA before irradiation,  $[\eta]_t$  – LVN of PLA after UV-irradiation during  $t$  time.

## Results and discussion

### General remarks

Poly(lactid acid) has been photochemically modified by creation of internal polymer network with three acrylate monomers: pentaerythritol triacrylate (PETA), pentaerythritol tetraacrylate (PETEA) or dipentaerythritol pentaacrylate (DPEPA). These monomers contain 3 (PETA), 4 (PETEA) and 5 (DPEPA) active groups capable to photopolymerization in the presence of initiator. The dry mixture of

PLA/acrylate (1:1) underwent very fast and efficient curing in few minutes UV exposure, resulting of which insoluble networks were formed. Although the conversion degree was not completed (60–90 %), the curing was stopped after 5 min to avoid photodegradation. It should be noted that alone PLA stays soluble during long term UV-irradiation, which clearly indicates that it does not undergo crosslinking.

Initially, the surfaces of samples were observed using optical microscope and the most representative places were chosen for AFM imaging. Two types of AFM images: topography and phase contrast obtained for pure PLA and PLA/acrylate networks (unexposed) and compared to images of the same samples after 2 h and 4 h UV-irradiation. Selected images are described below.

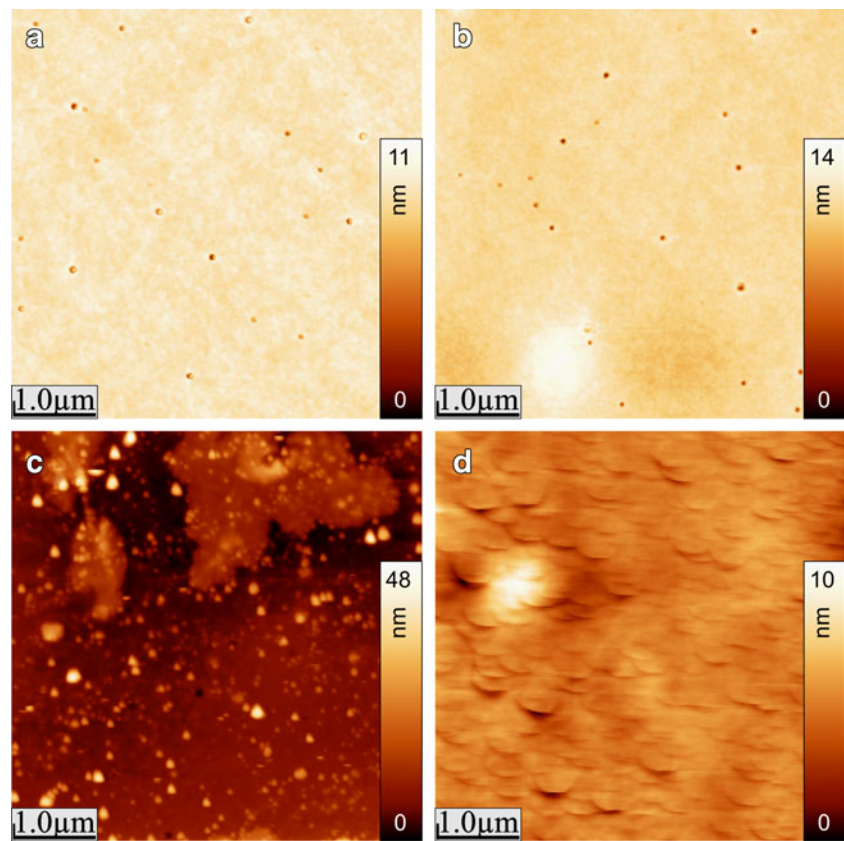
### AFM imaging of PLA

Figure 1 shows AFM images of PLA before and after exposure to UV at different times (0, 5 min, 2 and 4 h). As can be seen, untreated PLA has smooth surface ( $R_a=0.2$  nm) with some imperfections (circular depressions of about 100 nm of diameter, formed during fast solvent evaporation). Both topographic and phase contrast images indicate the relative homogeneity of PLA before exposure (Fig. 1a) and after 5 min of photocuring (Fig. 1b). It is confirmed by cross-section plots (Fig. 2). The roughness of PLA after 5 min is not changed significantly ( $R_a=0.3$  nm). The cross-sections show that the depressions become little bit deeper and broader (Fig. 2b).

After longer irradiation, PLA surface has been changed considerably (Figs. 1c, d, and 2c, d). Already 2 h of UV action leads to the formation of numerous small granules and higher surface heterogeneity. These granules are seen as a bright places. Theirs heights, estimated on the base of cross-section, are in 5–35 nm range. The roughness of 2 h irradiated PLA increases more than ten times comparing to unexposed sample (Table 1). Such modification of surface is probably caused by photodecomposition of macromolecules. The oligomers and low-molecular degradation products are formed as a result of random chain scission or abstraction of side methyl groups. Some of them can agglomerate at the surface creating the observed grains.

After 4 h UV-irradiation the further changes of PLA topography have been observed. The regular circular structures appearing at the whole PLA surface (Fig. 1d) may be considered as spherulites. PLA is a semicrystalline polymer, which means that both phases: amorphous and ordered exist together but the crystallinity degree depends strongly on the conditions of sample preparation [14, 15]. In the case of films prepared by solution casting and solvent evaporation, the crystalline phase is usually covered by thin amorphous layer. On the other hand, just the amorphous polymer is more sensitive to photodegradation than crystalline one

**Fig. 1** AFM topography images of poly(lactic acid) before irradiation (a), after 5 min (b), 2 h (c) and 4 h of UV-irradiation (d)



[16]. On the base of Fig. 1d, one can conclude that 4 h photodegradation was efficient enough to remove of this top layer. Thus, UV-irradiation acts as etching agent. The visible spherulite surface is rather smooth ( $R_a=0.4$  nm).

The formation of spherulitic structures as a result of molecular relaxation during exposure to UV should be also taken under consideration. The shorter chains formed during

PLA photodegradation are more mobile and they can attain more favorable, ordered conformations.

#### AFM imaging of polyacrylates

There were no possibility to get an image of the surface of monomers before curing because they are a viscous liquids.

**Fig. 2** Cross-sections of PLA surfaces presented in Fig. 1: before irradiation (a), after 5 min (b), 2 h (c) and 4 h of UV-irradiation (d)

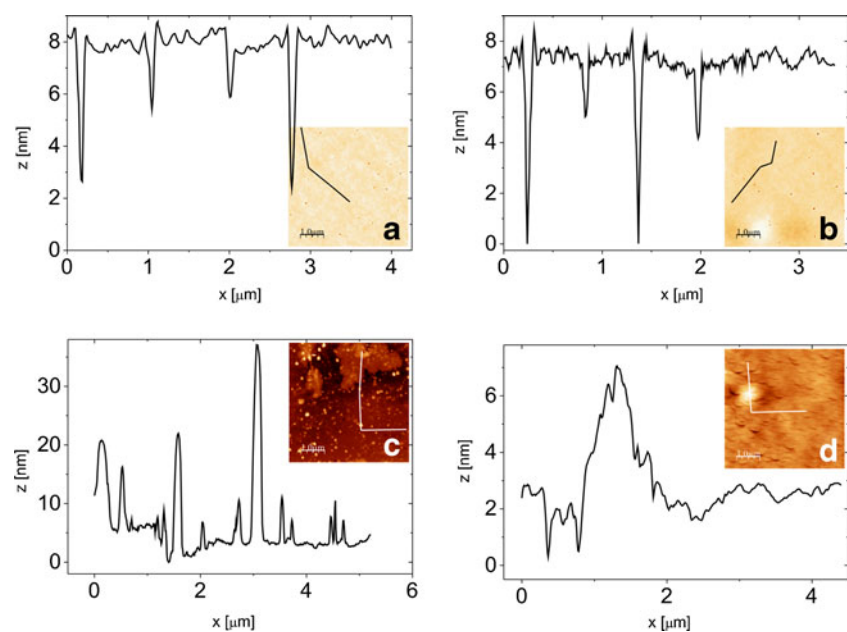




**Table 1** The roughness parameter ( $R_a$ , nm) of PLA and its composites with polyacrylates and the effect of UV-irradiation (calculated for  $5 \times 5 \mu\text{m}^2$  scanning area)

Sample	Time of UV-irradiation			
	0	5 min	2 h	4 h
PLA	0.2	0.3	3.0	0.4
PETA	-	0.3	0.3	0.2
PETEA	-	0.4	0.4	0.2
DPEPA	-	0.3	0.3	0.3
PLA+PETA	-	3.0	2.2	0.3
PLA+PETEA	-	8.0	0.3	0.6
PLA+DPEPA	-	14.7	2.3	5.8

Figure 3 presents the AFM images of three polyacrylates obtained from PETA, PETEA and DPEPA after 5 min photocuring and morphological changes after 4 h UV-

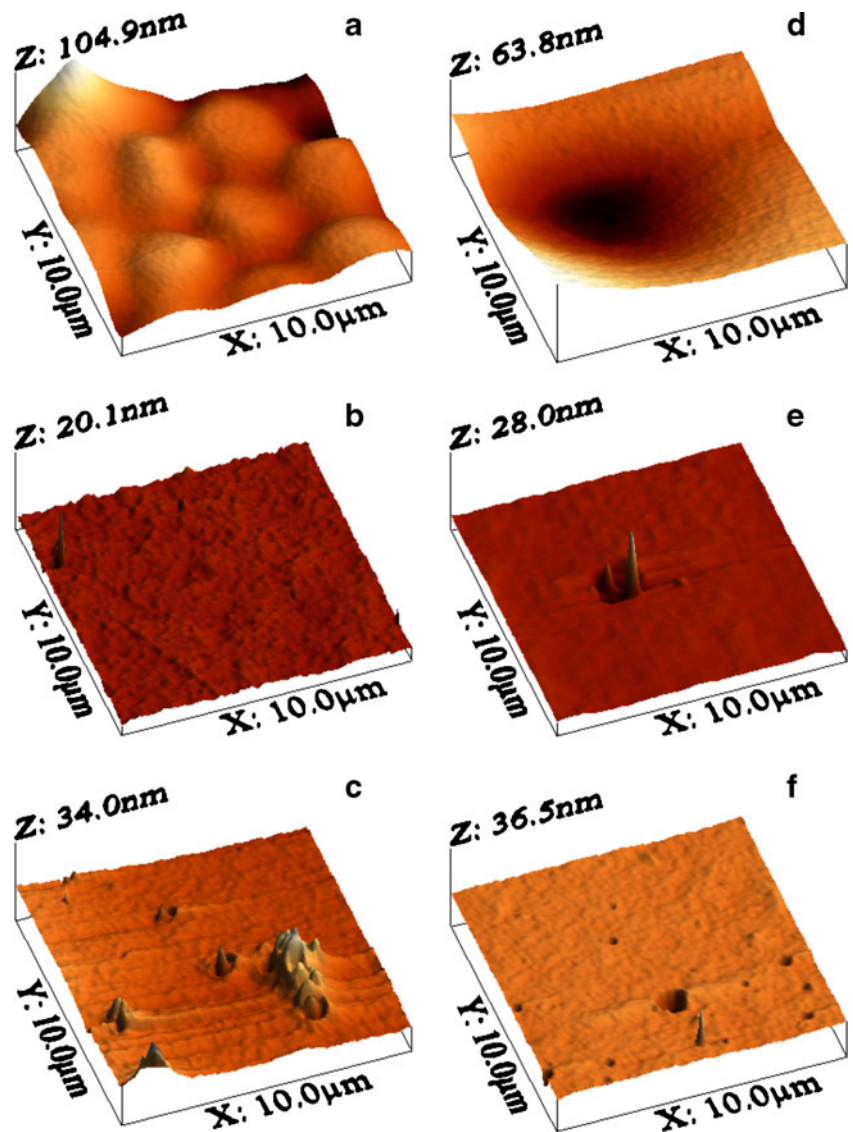
irradiation. All obtained polyacrylates are characterized by relatively low surface roughness, which does not change significantly after photodegradation (Table 1). However, the morphology of studied polyacrylates differs greatly.

The surface of poly(PETA) exhibits the coarse structure with grains size of about 2–4  $\mu\text{m}$  and this sample becomes smoother after UV-irradiation. The observed unevenness can be explained by shrinkage of material during fast polymerization, whereas smoothing upon UV is probably caused by efficient deterioration of protruding grains (Fig. 3a and d).

Poly(PETEA) surface is also relatively smooth and even more homogeneous than that in the case of poly(PETA). Tiny nodules are well distributed at whole surface (Fig. 3b).

The third polyacrylate – poly(DPEPA) exhibits the flat surface with relatively big imperfections seen in both topographic and phase contrast images (Fig. 3c). This monomer contains 5 functional groups in molecule and its polymerization is violent process, thus, the observed unhomogeneity

**Fig. 3** 3D-topographic images of polyacrylates: PETA (a), PETEA (b) and DPEPA (c) after 5 min photocuring (a–c, left column) and after 4 h photodegradation (d–f, right column)



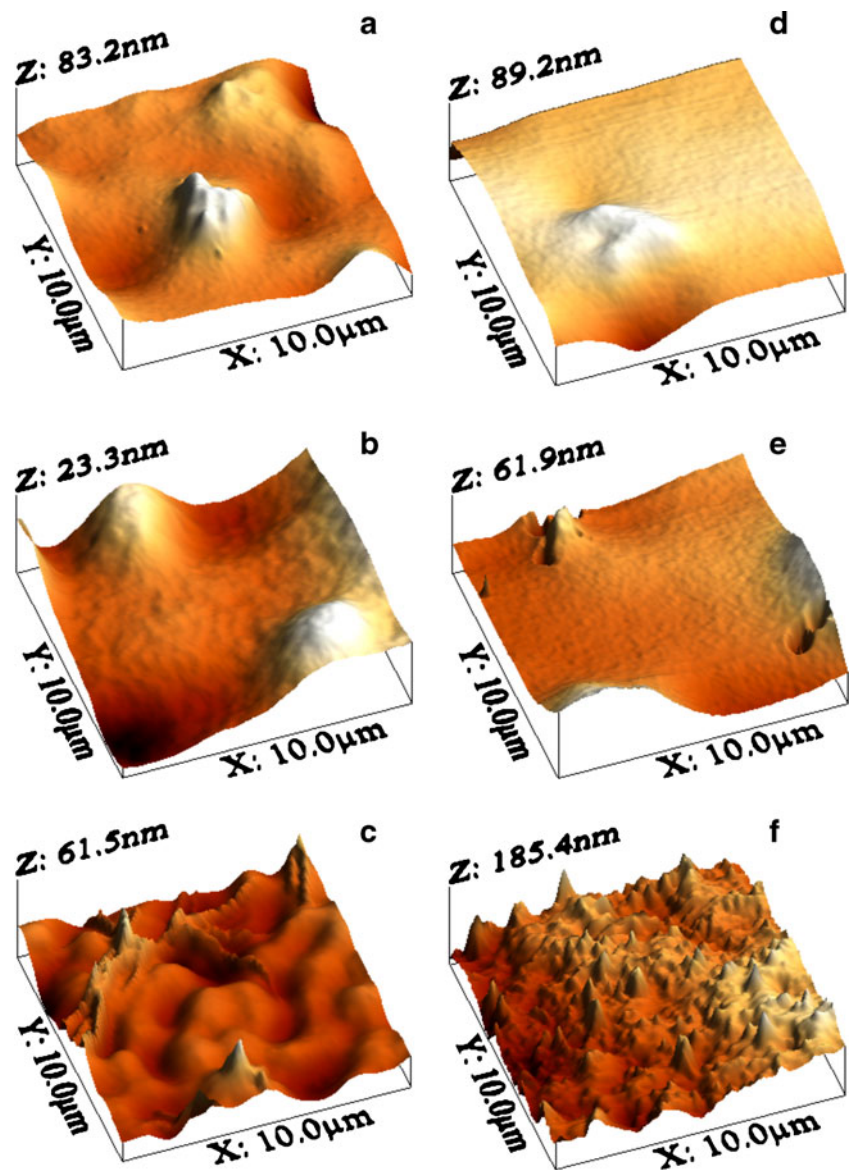
can be caused by the fast creation of local crosslinked network. Maybe the reaction occurs preferentially around the points where the initiator is accumulated.

Topographical changes in PETEA and DPEPA homopolymers after UV-irradiation are negligible (Fig. 3e and f). After 4 h UV- irradiation the highest changes in the surface topography among studied polyacrylates occurs in the case of poly(PETA). PETA molecule has three double bonds capable to reaction and this substrate was characterized by the fastest and most efficient photocuring [11]. Probably, during such rapid process, the numerous imperfections are created in composition structure.

#### AFM imaging of PLA/polyacrylate composites

Composites of PLA/polyacrylates are characterized by much higher surface roughness than pure PLA and polyacrylates

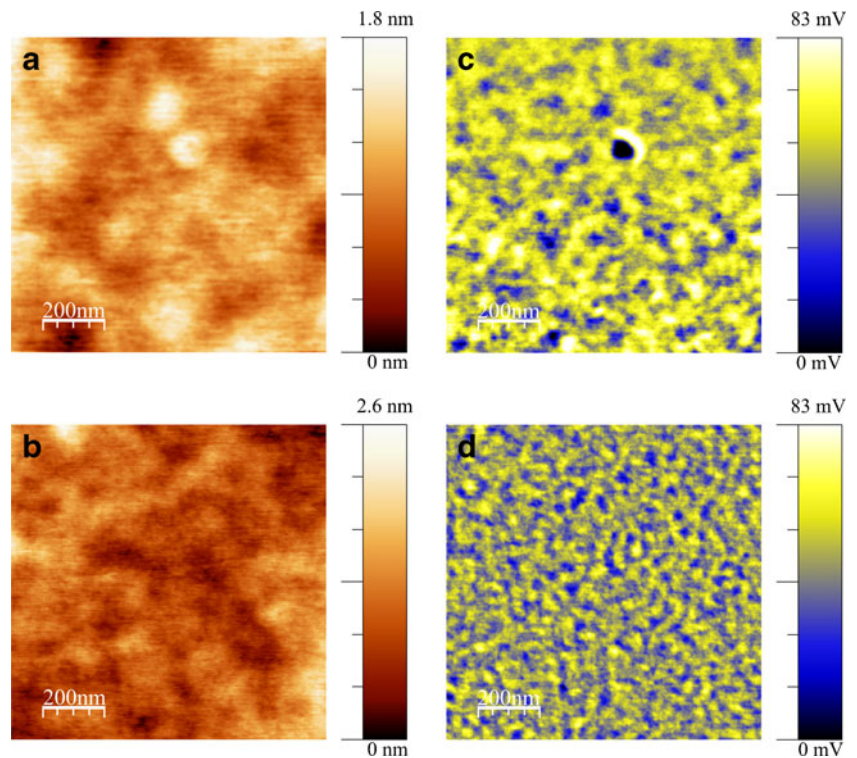
**Fig. 4** 3D-topographic images of composites: PLA+PETA (a, d), PLA+PETEA (b, e) and PLA+DPEPA (c, f) after 5 min of photocuring (a–c, left column) and after 4 h of photodegradation (d–f, right column)



alone (Table 1). The most representative images, typical for whole specimens surfaces, are presented in Fig. 4. The observed heterogeneity can be explained by the lack of miscibility of both components at molecular level. Interestingly, the surfaces in all these specimens undergo smoothing upon UV action.

An example of phase separation is shown in Fig. 5. Applied Intermittent-Contact Atomic Force Microscopy (IC-AFM) is very useful for topographical and compositional mapping due to high spatial and the minimal lateral interaction [17]. This operation mode is based on cantilever vibrations near the sample surface. The tip strikes the surface with sufficiently large amplitudes to eliminate its sticking to the surface. In IC-AFM mode, material composition mapping is performed by recording the shift between the cantilever excitation signal and photodetector signal [18]. This shift is known as a “phase signal” and depends on the

**Fig. 5** Topography (a, b) and corresponding phase images (c, d) of PLA+PETA after 5 min photocuring (a, c) and 4 h photodegradation (b, d)



energy dissipation during the tip–sample interactions [19]. Energy dissipation, in general, depends on local mechanical properties (elastic, viscoelastic and adhesive) of the sample surface. Image build from “phase signal” data is usually called as “material contrast” image. Phase imaging is commonly used to show material contrast in polymer blends and composites [10]. This method is very precise and it allows to detect the structures in composite materials in a nanometer range. It is clearly seen from Fig. 5c and d that PLA+PETA sample contains two separated phases which form the network of smaller structures than those observed in topography image (Fig. 5a and b). After 4 h UV-irradiation (Fig. 5d), these structures become even more tiny than untreated sample (Fig. 5c) due to partial surface photodegradation.

Particularly strong heterogeneity has been observed in PLA/poly(DPEPA). Some separated “islands” or “threads” are embedded in more or less homogeneous matrix (Fig. 6). They can be attributed to the separated phases of both polymers. The structure seen at Fig. 6b seems to be the initial but not perfect arrangement of macrochains, somewhat similar to those observed during spherulitic formation. Such “spherulite precursors” undergo gradual destruction upon UV-irradiation. Just after 2 h, instead of thread bundles, only residual short filaments are seen (Fig. 6c). Prolonged exposure (4 h) leads to complete decomposition of these structures observed at the sample surface. It indicates that the observed treads are composed of PLA because this

polymer is more photodegradable than polyacrylates. It results from the presence of ester groups in PLA backbone (in each polymer unit), which absorb UV-radiation and undergoes photolysis [20, 21]. Although poly(DPEPA) also contains acrylic (carbonyl) groups but there are side substituents, so their decomposition does not lead to such drastic changes in structure like those in the case of main chain scission in PLA. Moreover, poly(DPEPA) is highly crosslinked, contrary to linear PLA. It is well known that crosslinking (via covalent bonds) reinforces the polymer structure.

The size of these particular structures appearing randomly in this sample can be estimated from cross-sections (Fig. 6, right column). The largest “islands” are about 15  $\mu\text{m}$  broad and 280 nm height. The observed “treads” are thinner than 0.5  $\mu\text{m}$ .

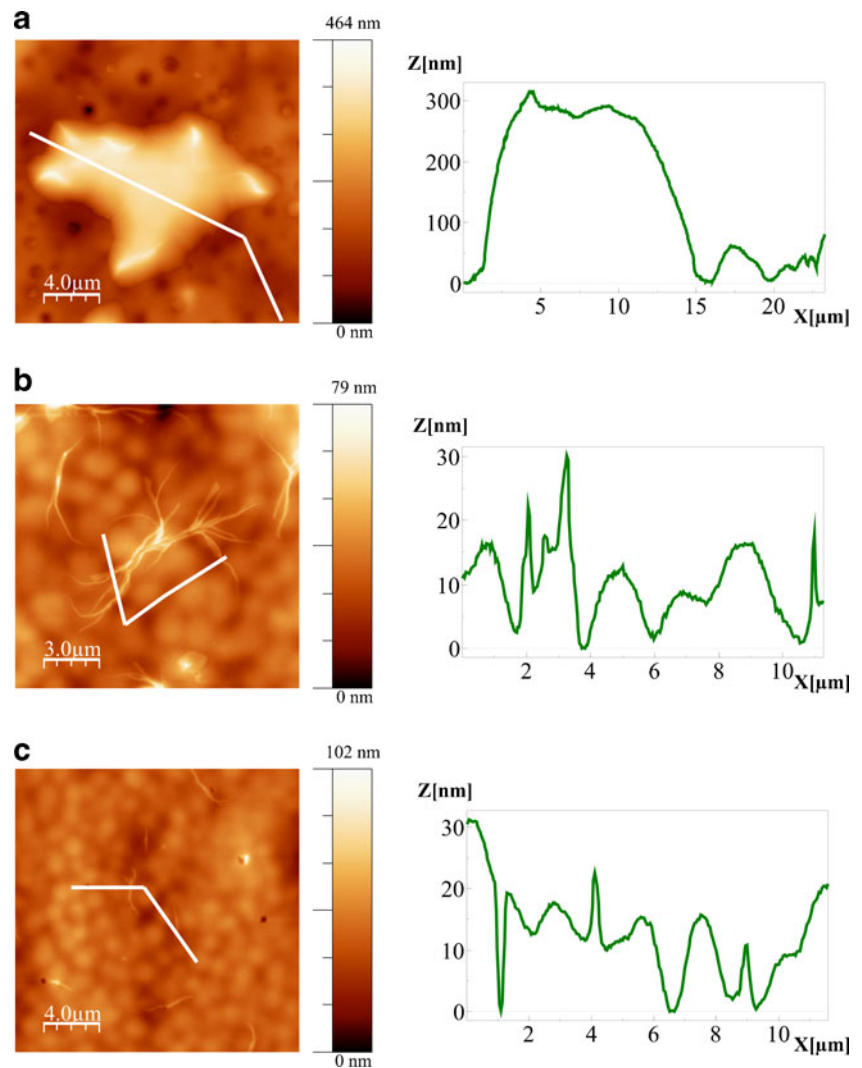
#### Differential scanning calorimetry

DSC experiments were performed for better explaining the composites morphology and to answer if the observed grains and protrusions on AFM images can be attributed to the crystalline phase of PLA. The high rate of heating or cooling (200  $^{\circ}\text{C}$ ) was used to detect the glass transition temperature ( $T_g$ ), which was invisible in the case of slow heating. DSC thermograms of studied samples are shown in Fig. 7.

Curve for virgin PLA shows  $T_g$  at 70  $^{\circ}\text{C}$  (obtained from the second run, Fig. 7a). It should be added that



**Fig. 6** Peculiarities of surface heterogeneity in DPEPA+PLA composite: **a)** phase separation, **b)** spherulite precursor, **c)** surface destruction after 2 h UV-irradiation



before polymer purification,  $T_g$  was lower (56 °C). Melting endotherm in PLA thermogram, occurring at 153 °C, confirms its semicrystalline nature but this peak is observed only at the first heating run. Moreover, the second small endothermic peak is also found at a higher temperature (170 °C). The cold crystallization has not been observed in this conditions. Similar results were described by Wang and Mano [14]. They found that the melting endotherm in DSC of PLA appeared only at a heating rate below 40°/min. The further decrease of heating rates allows observation of double cold crystallisation peaks. They concluded that the heating rate could significantly influence cold crystallisation in PLA.

It is necessary to point out that the first heating curve contains the additional peak due to relaxation processes, which partially overlaps to the glass transition.

The nature of double crystalline peaks has been discussed in literature [22–24]. One assumes that it can be

the result of lamellar rearrangement [22] or that different types of crystallinities are formed (more and less perfect structures of various sizes) [23, 24]. Other explanations concern the crystallization from different amorphous regions (inter-spherulites or inter-lamellar) as well as simultaneous formation of metastable and highly stable ordered phases [14].

Pure acrylate cured monomers do not exhibit any characteristic  $T_g$  in studied conditions (thermograms non-shown), despite the high heating rate. Certainly, the reason is the high rigidity of almost fully cross-linked polyacrylates (the amount of insoluble gel extracted from network is approximately 100 % in all three cases: polyPETA, polyPETEA and polyDPEPA) [11]. In PLA/polyacrylate networks,  $T_g$  somewhat exceeds 70 °C. It means that polyacrylates crosslinked in PLA stiffens the matrix to some extent.

In the presence of polyacrylate, the melting temperature decreases to 138 °C and 136 °C in PETA+PLA



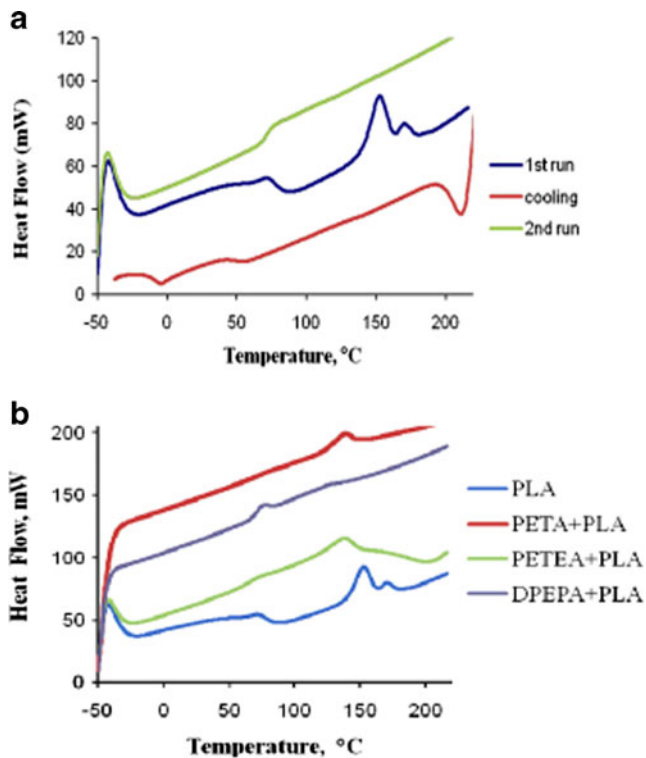


**Fig. 7** DSC thermograms of pure PLA (a) and PLA/polyacrylate composites (b)

and PETEA+PLA, respectively (Fig. 7b, Table 2). It indicates that PLA crystallinities in these blends are quite different or less perfect than those in PLA alone. It can be explained by fastly formed network of polyacrylates, which hampers the crystallization process. In highly crosslinked systems the segmental movement, needed for arrangement and building of regular, ordered structure is restricted. Moreover, the fragments of polyacrylate chains (PETA and PETEA) entangled with PLA act as “impurities” decreasing  $T_m$ .

However, in the third formulation (DPEPA+PLA) there is no clear peak in this range. It suggests that in the presence of five-functional monomer, which has highly branched

**Table 2** Melting temperature ( $^{\circ}\text{C}$ ) of PLA and its composites (estimated from the first heating run on DSC curve)

Sample	$T_m(1)$	$T_m(2)$
PLA	153	170
PLA+PETA	138	-
PLA+PETEA	136	-
PLA+DPEPA	-	-
PLA+PETA+PEG	103	142
PLA+PETEA+PEG	103	137
PLA+DPEPA+PEG	-	-

structure, the crosslinking during film formation is faster than crystallization process.

The fast cooling and heating at the second run cause formation of amorphous films (lack of endothermic peaks in thermograms of all samples), which is understood because formation of crystalline phase strongly depends on the conditions of film preparation and the thermal history of the sample.

#### X-ray diffraction

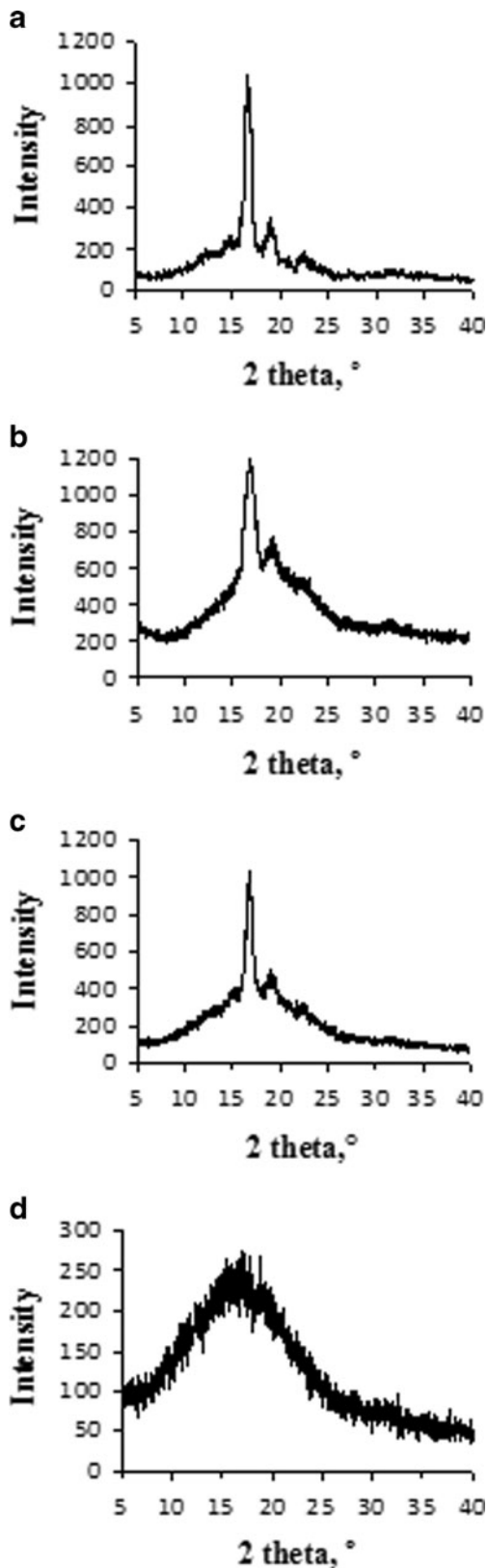
As it was shown above, PLA is able to form crystalline phase, which disappears after fast thermal treatment. For AFM studies, the networks were prepared at room temperature, thus, the presence of crystallinities in those samples can be expected. To confirm this supposition, additionally the XRD analysis has been done.

Figure 8 shows the XRD patterns of all studied samples. Pure PLA (Fig. 8a) exhibited characteristic peaks at  $2\theta = 12.5, 14.7, 16.6, 19.1^{\circ}$  and  $22.3^{\circ}$  which coincided with the data published previously [25–27]. The main peak at  $16.6^{\circ}$  corresponds to interplanar spacing of  $5.9 \text{ \AA}$  [27]. Such PLA pattern is characteristic for orthorhombic form containing 20 units in the crystalline cell [28].

The diffractograms of PETA+PLA and PETEA+PLA (Fig. 8b and c) have the signals at the same value of  $2\theta$  as PLA, but their intensity is obviously lower. Notwithstanding, DPEPA+PLA has only broad band characteristic for amorphous polymer, which is in agreement with DSC results. Comparing to AFM observation it can be concluded that this amorphous specimen formed very rough surface contrary to smoother surfaces of partially crystalline samples (PLA+PETA and PLA+PETEA). These observations are in well accordance with the described above DSC results.

It should be added that in spite of crystallinity in PLA+PETA and PLA+PETEA detected by XRD (Fig. 8b and c), there were no spherulitic structures on AFM images (Fig. 4d and e). This difference is understandable because XRD concerns the results for whole volume of sample, contrary to AFM showing only the surface image.

The comparison of results obtained from both techniques: XRD and AFM allows to conclude that ordered crystalline phase in composites of PLA+PETA and PLA+PETEA is placed in deeper, internal layers of films. However, UV-irradiation leads to destruction of crystallinities in these blends. XRD patterns of exposed PLA+PETA and PLA+PETEA for 4 h (non-shown here) shows broad amorphous halo, typical for lack of crystallinity. Pure PLA behaves in different way: XRD signals are present after UV exposure but their intensity is somewhat lower. Looking at the AFM image (Fig. 1d) we observed the removing of top amorphous layer and revealing of spherulitic surface.



**Fig. 8** XRD patterns of pure PLA (a) and its composites: PETA+PLA (b), PETEA+PLA (c) and PLA+DPEPA (d)

### Changes of PLA molecular weight measured by viscometry

Classic viscometry has been applied for monitoring the photodegradation process in PLA. Limiting viscosity number (LVN) of initial PLA equals 3.15 dl/g which corresponds to viscosity average molecular weight  $M_v = 2.48 \cdot 10^5$ . LVN values were applied for calculation of chain scission number per one macromolecule (S), defined in experimental part.

The decrease of LVN and  $M_v$  indicates that the random chain scission takes place in PLA upon UV-irradiation (Table 3). The rapid drop of average molecular weight was observed just during first hour of UV action. However, less than one crack per molecule (S) was found at this time. Prolonged exposure caused the fast progress of PLA degradation. Finally, after 4 h UV-irradiation, the  $M_v$  was reduced over 4 times and corresponding S value increases to above 3.

Observed photodegradation is obviously initiated by photon absorption and excitation of macromolecules. In PLA, mainly carbonyl groups and possible structural defects are responsible for the light absorption. The excess of energy is consumed in the chemical reactions of bond breaking, what is proved by discussed above viscometry results. The main photochemical processes in polyesters, leading to the reduction of chain length, are Norrish I and II type reactions, described elsewhere [16]. The lack of linearity of S changes versus exposure time suggests that besides chain scission, other competitive reactions occurs. In the case of pure PLA, no insoluble gel was formed, which excludes photocrosslinking.

The small amount of soluble PLA fraction has been extracted from UV-irradiated composites with polyacrylates. We have obtained only 3 wt%, 6wt % and 11 wt % from PLA/polyPETA, PLA/polyPETEA and PLA/polyDPEPA composite, respectively. Such small amount of soluble part proves that PLA, which does not undergo photocrosslinking, has to participate in propagation step

**Table 3** Changes of limiting viscosity numbers (LVN), viscosity average molecular weight ( $M_v$ ) and number of chain scission (S) in UV-irradiated PLA

Irradiation time, h	LVN, mol/g	$M_v$ , g/mol	S <sup>a</sup>
0	3.15	$2.48 \cdot 10^5$	0
0.5	2.10	$1.46 \cdot 10^5$	0.69
1	2.10	$1.37 \cdot 10^5$	0.80
2	1.55	$0.98 \cdot 10^5$	1.51
3	1.45	$0.90 \cdot 10^5$	1.74
4	1.00	$0.58 \cdot 10^5$	3.33

<sup>a</sup>  $S = ([\eta]_0 / [\eta]_t)^{1/\alpha} - 1$ , where:  $[\eta]_0$  – LVN of PLA before irradiation,  $[\eta]_t$  – LVN of PLA after UV-irradiation during  $t$  time

of acrylate polymerization (for example, in chain transfer leading to grafted copolymer). Moreover, the physical entanglement of PLA macromolecules in three dimensional network of polyacrylate also makes impossible extraction of it.

The PLA/polyDPEPA contained the higher amount of soluble PLA comparing to two other samples. It can be explained by very fast photocuring as a result of simultaneous reaction of five functional groups. Generally, the higher number of reactive groups in monomer particles leads to an increase of polymerization rate [29, 30]. Even autoacceleration is observed in photocuring of multifunctional acrylates. However, after first violent step, the process slow down because the propagation is diffusion-controlled. Thus, restriction of mobility of reacted macroradicals due to their trapping in cross-linked network causes their diffusion difficult. The trapping of radicals in network is enhanced by the strong shrinkage of specimen during very fast step at the beginning reaction. In effect, the monomer conversion is retarded or even stopped and the reaction yield is lower than it could be expected.

Measured viscosity of soluble fractions allows for the determination of molecular weight changes caused in PLA by photodegradation (Fig. 9). The drop of  $M_v$  (expressed as percentage changes) is very small after short irradiation (0.5–2 h) but significant after 4 h of exposure. Interestingly, the  $M_v$  changes (as well as numbers of chain scission) of PLA photodegraded in the blend are lower than in the case of PLA exposed separately. This proves that formed composites are characterized by very good photostability, much better than PLA alone.

In composites, the most efficient degradation of PLA has been observed in the presence of DPEPA, which can be explained by the lack of macromolecular order (Fig. 8d) and the lowest amount of gel in this sample [11].

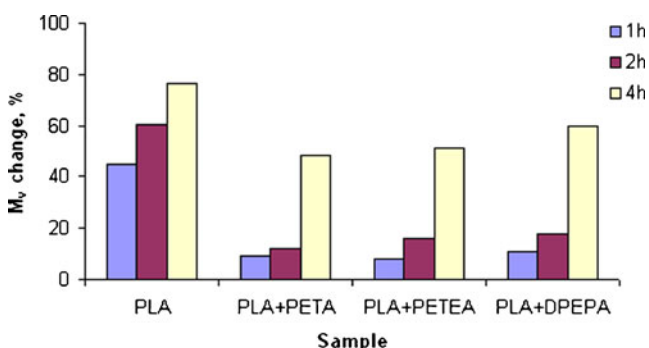


**Fig. 9** Negative changes of viscosity average molecular weights (%) in PLA and its composites after UV-irradiation

## Conclusions

PLA film is the most homogenous among studied samples but its amorphous part is sensitive to photodegradation. UV-radiation acts as etching agent removing the most top layer and displaying the ordered interior i.e. PLA spherulities.

Pure polyacrylates form smooth, relatively homogenous surfaces, which are resistant to UV-irradiation. PLA/polyacrylate (1:1) are characterised by higher roughness and phase separation but they undergo partial smoothing after exposure to UV. The different topographies dependent on composition were observed.

PLA/polyacrylates networks are more photostable than PLA alone. It is mainly caused by the high crosslinking degree of these blends. The PLA/DPEPA is most photosensitive among compositions studied which is caused by the lack of PLA crystallinity and lowest crosslinking degree in this case.

The photoresistance of PLA in the blends, important in the case of practical applications, can be significantly improved by the simple, fast and safe method of multifunctional monomer photocrosslinking. Possibility of such chemical modification makes this material an interesting candidate in the future packaging technology.

**Open Access** This article is distributed under the terms of the Creative Commons Attribution License which permits any use, distribution, and reproduction in any medium, provided the original author(s) and the source are credited.

## References

- Gupta B, Revagade N, Hilborn J (2007) Poly(lactic acid) fiber: an overview. *Prog Polym Sci* 32:455–482
- Duda A, Penczek S (2003) Polilaktyd [poli(kwas mlekowy)]: synteza, właściwości zastosowania. *Polimery* 48:16–27
- Rasal R, Janorkar AV, Hirt DE (2010) Poly(lactic acid) modifications. *Prog Polym Sci* 35:338–356
- Nieddu E, Mazzucco L, Gentile P, Benko T, Balbo V, Mandrile R, Ciardelli G (2009) Preparation and biodegradation of clay composites of PLA. *React Funct Polym* 69:371–379
- Borcia C, Borcia G, Dumitrasc N (2008) Relating plasma surface modification to polymer characteristics. *Appl Phys A90*:507–515
- Bhattacharya A, Rawlins JW, Ray P (2009) Polymer grafting and crosslinking. John Wiley & Sons, New Jersey
- Kaczmarek H, Drag R, Świątek M, Oldak D (2002) The influence of UV-irradiation on poly(vinyl chloride) modified by poly(vinyl acetate). *Surf Sci* 507:877–882
- Baltá-Calleja FJ, Fakirov S (1997) Recent advances in the study and characterization of polymers by microhardness. *TRIP* 5:246
- Kaczmarek H, Galka P (2011) Nano-mechanical properties of modified poly(methyl methacrylate) films studied by atomic force microscopy. *Tribol Lett* 41:541–554
- Achalla P, McCormick J, Hodge T, Moreland C, Esnault P, Karim A, Raghavan D (2006) Characterization of elastomeric

- blends by atomic force microscopy. *J Polym Sci B Polym Phys* 44:492–503
11. Kaczmarek H, Vuković-Kwiatkowska I (2012) Preparation and characterization of interpenetrating networks based on polyacrylates and poly(lactic acid). *eXPRESS Polym Lett* 1:78–94
  12. Horcas I, Fernandez G, Gomez-Rodriguez JM, Colchero J, Gomez-Herrero J, Baro AM (2007) WSXM: a software for scanning probe microscopy and a tool for nanotechnology. *Rev Sci Instrum* 78:013705(1–8)
  13. Proikakis C, Mamouzelos NJ, Tarantili PA (2006) Swelling and hydrolytic degradation of poly(D, L-lactic acid) in aqueous solutions. *Polym Degrad Stab* 91:614–619
  14. Wang Y, Mano JF (2005) Role of thermal history on the thermal behavior of poly(L-lactic acid) studied by DSC and optical microscopy. *J Therm Anal Calorim* 80:171–175
  15. Vasanthan N, Ly O (2009) Effect of microstructure on hydrolytic degradation studies of poly(L-lactic acid) by FTIR spectroscopy and differential scanning calorimetry. *Polym Degrad Stab* 94:1364–1372
  16. Rabek JF (1996) Photodegradation of polymers. Physical characterization and applications. Springer, Berlin
  17. Klinov D, Magonov S (2004) True molecular resolution in tapping-mode atomic force microscopy with high-resolution probes. *Appl Phys Lett* 84:2697–2699
  18. Garcia R, Magerle R, Perez R (2007) Nanoscale compositional mapping with gentle forces. *Nat Mater* 6:405–411
  19. Cleveland JP, Anczykowski B, Schmid AE, Elings VB (1998) Energy dissipation in tapping-mode atomic force microscopy. *Appl Phys Lett* 72:2613–2615
  20. Yasuda N, Wang Y, Tsukegi T, Shirai Y, Nishida H (2010) Quantitative evaluation of photodegradation and racemization of poly(lactic acid) under UV-C irradiation. *Polym Degrad Stab* 95:1238–1243
  21. Hideto T, Sugiyama H, Sato Y (2012) Photodegradation of poly(lactic acid) stereocomplex by UV-irradiation. *J Polym Environ* 20:706–712
  22. Nijenhuis AJ, Colstee E, Grijpma DW, Pennings AJ (1996) High molecular weight poly(L-lactide) and poly(ethylene oxide) blends: thermal characterization and physical properties. *Polymer* 37:5849–5857
  23. Kulinski E, Piotrowska E (2005) Crystallization, structure and properties of plasticized poly(L-lactide). *Polymer* 46:10290–10300
  24. Li J, Che D, Gui B, Gu M, Ren J (2011) Crystallization morphology and crystallization kinetics of poly(lactic acid): effect of *N*-Aminophthalimide as nucleating agent. *Polym Bull* 67:775–791
  25. Piotrowska E, Kulinski Z, Galeski A, Masirek R (2006) Plasticization of semicrystalline poly(L-lactide) with poly(propylene glycol). *Polymer* 47:7178–7188
  26. Carrasco F, Pagès P, Gámez-Pérez J, Santana OO, Maspoch ML (2010) Processing of poly(lactic acid): characterization of chemical structure, thermal stability and mechanical properties. *Polym Degrad Stab* 95:116–125
  27. Brizzollara D, Cantow HJ, Diederichs K, Keller E, Domb A (1996) Mechanism of the stereocomplex formation between enantiomeric poly(lactide)s. *Macromolecules* 29:191–197
  28. Miyata T, Masuko T (1997) Morphology of poly(L-lactide) solution-grown crystals. *Polymer* 38:4003–4009
  29. Kaczmarek H, Decker C (1994) Interpenetrating polymer networks. I. Photopolymerization of multiacrylate systems. *J Appl Polym Sci* 54:2147–2156
  30. Kaczmarek H, Oldak D, Szalla A (2002) Networks of photocrosslinked poly(methacrylates) in linear poly(vinyl chloride). *J Appl Polym Sci* 86:3725–3734